Identification of typical eco-hydrological behaviours using InSAR allows landscape-scale mapping of peatland condition

Andrew V. Bradley[1], Roxane Andersen[2], Chris Marshall[2], Andrew Sowter[3], David J. Large[4]

[1]Department of Chemical and Environmental Engineering, Faculty of Engineering, Nottingham Geospatial Institute, Innovation Park, Jubilee Campus, Nottingham, NG7 2TU, UK
[2]Environmental Research Institute, University of Highlands and Islands, Castle Street, Thurso, Scotland, KW14 7JD, UK
[3]Terra Motion Limited, Ingenuity Centre, Innovation Park, Jubilee Campus, University of Nottingham, Nottingham. NG7 2TU, UK
[4]Department of Chemical and Environmental Engineering, Faculty of Engineering, University of Nottingham, Nottingham. NG7 2RG, UK

Correspondence to: Andrew V. Bradley (andrew.bradley1@nottingham.ac.uk)

Abstract. Better tools for rapid and reliable assessment of global peatland extent and condition are urgently needed to support action to prevent their further decline. Peatland surface motion is a response to changes in the water and gas content of a peat body regulated by the ecology and hydrology of a peatland system. Surface motion is therefore a sensitive measure of ecohydrological condition but has traditionally been impossible to measure at the landscape scale. Here we examine the potential of surface motion metrics derived from InSAR satellite radar to map peatland condition in a blanket bog landscape. We show that the timing of maximum seasonal swelling of the peat is characterized by a bimodal distribution. The first maximum usually in autumn is typical of 'stiffer' peat associated with steeper topographic gradients, peatland margins, degraded peatland and more often associated with 'shrub' dominated vegetation communities. The second maximum usually in winter is typically associated with 'softer' peat typically found in low topographic gradients often featuring pool systems and *Sphagnum* dominated vegetation communities. Specific conditions of 'soft' and 'stiff' peats are also determined by the amplitude of swelling and multi-annual average motion. Peatland restoration currently follows a re-wetting strategy; however, our approach highlights that landscape setting appears to determine the optimal endpoint for restoration. Aligning expectation for restoration outcomes with landscape setting might optimise peatland stability and carbon storage. Importantly, deployment of this approach, based on surface motion dynamics, could support peatland mapping and management on a global scale.

1. Introduction

The conservation of well-functioning peatlands and restoration of degraded peatlands, to reduce and ultimately mitigate land-use related emissions of atmospheric carbon dioxide, is now a global priority (Leifeld and Menichetti, 2018; Amelung et al., 2020; Günther et al., 2020). Furthermore, to support the implementation of national peatland management plans and restoration initiatives, cost-effective measures to record current peatland condition and restoration progress are urgently required (Crump, 2017). Mapping peatland extent and condition has long been recognized as a huge challenge over large, remote, wet, and often

discontinuous peat forming regions where field-based surveys are impractical and expensive (Lees et al., 2018). Alternatives such as thematic mapping based on optical remote-sensing (visible and near-infra red) are increasingly used (Artz et al., 2018; Minasny et al., 2019; Lees et al., 2020), but the number of observations in regions with frequent cloud cover such as peatland

35   in the northern latitudes and the tropics reduces the number of possible surface observations. Radio detection and ranging (Radar) that is sensitive to physical properties of the surface, provides an effective, more frequent option, given that microwave frequencies can penetrate cloud cover and return a measured signal from the ground (Minasny et al., 2019; Poggio et al., 2014). For example, using the ESA Sentinel-1 Synthetic Aperture Radar (SAR) satellites it is now possible to observe a peatland surface anywhere at high frequency (6 to 12 days) with continuous spatial coverage. When this is combined with the technique

40   of SAR Interferometry (InSAR) it allows detection of surface displacement, an indication of peatland condition, as a time-series of observations (Sowter et al., 2013).

In peatland, the rise and fall of the surface, sometimes described as 'bog-breathing' (Kulczynski, 1949; Baden and Eggelsmann, 1964; Mustonon and Suena, 1971; Hutchinson, 1980; Kurimo, 1983; Almendinger et al., 1986; Price, 2003; Price and Schlotzhauer, 2003), is one of the key self-regulating feedback mechanisms in peatland, providing resilience and maintaining

45   function during periods of hydrological stress (Money and Wheeler, 1999; Waddington et al., 2015; Mahdiyasa et al., 2021). This 'surface motion', which is a poro-elastic mechanical response to ecohydrological processes, results from the collapse and expansion of large pores in response to changes in the mass of water stored and associated stresses within the peat (Price, 2003; Mahdiyasa et al., 2021). Mechanical deformation of the peat body and consequent surface motion can also modify the ecohydrology of a peatland via compaction, slope failure and pipe formation (Waddington et al., 2010; Waddington et al.,

50   2015). Small-scale field observations indicate that peat surface motion is influenced by changes in water level (Roulet, 1991; Price, 2003; Kennedy and Price, 2005; Fritz at al., 2008; Alshammari et al., 2020), vegetation composition (Howie and Hebda, 2018; Alshammari et al., 2020), micro-topography (Waddington et al., 2010), accumulation and upward migration of methane bubbles (Glaser, et al., 2004; Reeve et al., 2013) and land management (Kennedy and Price, 2005).

Collectively these results suggest that peatland surface motion could be a sensitive indicator of peatland function on a landscape

55   scale. So far, InSAR investigations have focused on discrete, small-scale (<1 km^2) peatlands (Fiaschi et al., 2019; Tampuu et al., 2020), identifying the potential range in timing and amplitude of seasonal peatland surface motion (Alshammari et al., 2018; Alshammari et al., 2020) and its relationship to precipitation (Fiaschi et al., 2019), water level (Alshammari et al., 2020; Tampuu et al., 2020) and vegetation composition (Alshammari et al., 2020). However, peatland landscapes contain a continuum of topographic, ecological, hydrological and management regimes and these small-scale studies have not captured

60   the full spectrum of peatland conditions between degraded and near natural.

In this paper, we determine whether surface motion measured by InSAR can be used to quantify peatland condition continuously over a complex peatland landscape. Using the APSIS (Advanced Pixel System using Intermittent Small Baseline Subset, formerly known as the Intermittent Small Baseline Subset (ISBAS)) method, which is capable of generating spatially continuous measures of vertical surface motion over peatland (Sowter et al., 2013), we measure time series of surface motion

65   over our study site at a high spatial and temporal resolution. Specific time series metrics are then compared to independent measures of peatland condition to determine their relationship. By doing this we relate surface motion metrics to the continuum of ecohydrological conditions in this peatland landscape. Finally, we demonstrate how surface motion metrics can be used to map the ecohydrology of a peatland system. By doing so we illustrate how our new approach could be applied to monitoring the response of global peatland to restoration, management, and climate change.

2. Study Location

70

The Flow Country peatlands, Northern Scotland (Andersen et al., 2018) exist in a range of topographic, hydrological and management settings, leading to a range of different conditions e.g., highly eroded uplands to relatively intact low-lying peatland with pool systems, superimposed by activities such as forestry, drainage, and grazing. Our chosen study site is 930 km^2 of blanket bog, ranging from 50 to 600 m.a.s.l (Fig. 1). From the 19th century onwards, management has involved burning

75   to support grouse shooting and artificial drainage of the driest areas of peatland, targeted for subsidized agricultural improvement and later afforestation programs (Sloan et al., 2018). More recently, near-natural areas have been designated for conservation (Lindsay et al., 1988), and previously afforested and drained areas started undergoing restoration. Some areas are also actively eroding, particularly at the highest altitudes (Hancock et al., 2018). This complex mosaic of near-natural and modified peatlands makes the study site particularly suited to an investigation on the use of InSAR for mapping peatland

80   condition. To understand the variation and distribution in the characteristics of the APSIS derived time series, we analysed five well-documented 10 to 15 km^2 sub-sites within the study area (Table 1; Fig. 1).
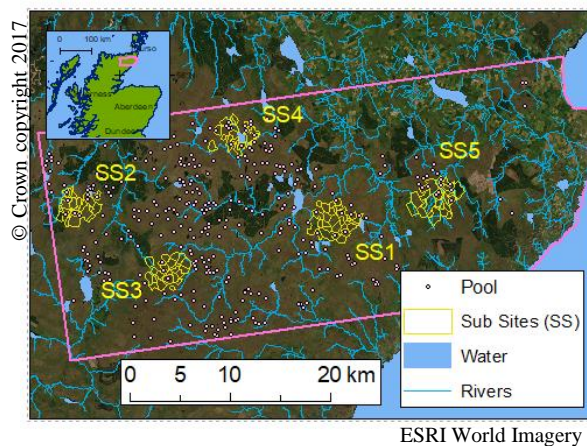
Figure 1: The study location (inset) and study area, outlined, in the Flow Country, Northern Scotland. Forested areas are dark green, with the main river network and location of pool features shown with sub-sites for detailed analysis marked as SS1 to SS5.
85   **Credits: ERSI World Imagery, sources ESRI, DigitalGlobe, GeoEye, i-cubed, USDA FSA, USGS, AEX, Getmapping, Aerogrid, IGN, IGP, swisstopo, and the GIS User Community, © Crown copyright 2017. Distributed under the Open Government Licence (OGL). Ordnance Survey (Digimap Licence).**

Table 1: Details of the five sub-sites (SS), which are all currently designated as Site of Special Scientific Interest (SSSI), Special Protection Areas (SPA) and Special Areas of Conservation (SAC).

SS	1	2	3	4	5
Name	Balavreed	Cross Lochs	Knockfin	Loch Caluim	Munsary
Location	58.38N -3.50E	58.39N -3.94E	58.32N -3.80E	58.44N -3.68E	58.39N -3.35E
Altitude (m.a.s.l)	~180	~180	~360	~120	~100
Topography	Watershed, gently undulating with pool systems	Flat pool systems on watershed with steep slopes into a valley	Eroding upland ridge with pools, ephemeral pools, and hags (wind eroded peat islands)	Gently sloping basin into central loch	Gently undulating area incised by small streams
General condition	Near-natural	Near-natural, drier peat	Eroding peat	Near-natural	Near-natural including agriculture and forestry
Current management	Low level sheep and deer grazing, conservation	Low to medium grazing by deer. Includes	Deer grazing, Forestry to the north and drainage to the	Low level sheep and deer grazing, under conservation	Intense drainage for agriculture and grazing surrounded by

	management agreement	restoration (forest-to-bog and drain blocking) areas. Conservation management as part of Forsinard Flows National Nature Reserve (FFNNR)	East. Conservation management as part of FFNNR	management agreement with FFNNR	forestry and forestry to bog to east and South. Part of the site under conservation management by Plantlife Scotland.
History	Evidence of damage from historic burning, peat cutting and drainage (hill drains) in places alongside natural drainage lines.	Surrounded by restoration areas (forest-to-bog undertaken in 2006) and standing forestry on deep peat. Wildfire in 1981	The surrounding areas have been drained and burnt in the past.	Some historic drainage and peat cutting. The area was also historically used for cattle grazing and is part of an old drove road.	Historic drain blocked with plastic piling in 2003. Historic drainage and burning.

3 Materials and Methods

3.1 InSAR and time series preparation

InSAR surface motion time series were calculated at a pixel resolution of 80 x 90 m across the study site. To calculate the surface motion, we used 410 Sentinel–1A and –1B synthetic aperture radar images (descending orbit 125) gathered every 6 to 12 days between March 12th 2015 and July 1st 2019 from the European Space Agency Copernicus Open Access Hub (https://scihub.copernicus.eu). Satellite interferometry was applied using these images with the APSIS technique (Sowter et al., 2013). The APSIS technique contains an adapted version of the established SBAS Differential InSAR time series algorithm (Bateson et al., 2015; Cigna and Sowter, 2017). It was designed to improve the density and spatial distribution of survey points to return measurements in vegetated areas, where Differential InSAR processing algorithms habitually struggle due to incoherence (Osmanoğlu et al., 2016; Gong et al., 2016). The APSIS algorithm was implemented using Terra Motion Limited's in-house Punnet software, which covers all aspects of processing from the co-registration of SLC (Single Look Complex) data to the generation of time series (Sowter et al., 2016). Standard interferometry image thresholds were: maximum horizontal baseline no more than 250m, a maximum temporal separation of 1 year between image pairs using a coherence threshold of 0.25, and a minimum multi-look point acceptance threshold of 360 to a resolution of 80 by 90 m. Motion was measured relative to a stable reference point, a building on glacial till, at Wick Airport (58.4533° N, 3.0879° W). Phase unwrapping was implemented using an in-house implementation of the Statistical-cost, Network-flow Algorithm for Phase Unwrapping (SNAPHU; Chen and Zebker, 2001). Two products were produced for each georeferenced pixel location, the multi-annual average velocity (m yr^{-1}) of the time series calculated from the radar line-of-sight, and the 6 - 12 day time series of surface motion that detects the seasonal expansion and contraction (or bog breathing) as annual oscillations in relative height (Alshammari, et al., 2018). Each motion time series was then processed as follows:

First, using the R programming environment (R Core Team, 2013), the time series was sub-sampled into equal time intervals of 12 days, to match the longest overpass interval of Sentinel–1 images since Sentinel-1B, which reduces overpass times to 6 days, was not operational until 2016. Outliers were re-estimated using the R 'tsclean' function (Box and Cox, 1964), from R package 'Forecast' (Hyndman et al., 2020). Gaps were filled with a linear interpolation using the R 'approx' function (Becker et al., 1988) from R 'stats' package (R Core Team, 2020) after 'spline' interpolation methods were found to produce contradictory results with adjacent time series across the largest gaps. The 'detrend' R function aligned and reset each time series around zero by subtracting the mean.

Second, Multichannel Singular Spectrum Analysis (MSSA) using the SSA-MTM toolkit (Ghil et al., 2002; SPECTRA, 2021) was applied to isolate the cyclical, annual seasonal component of the time series from regional climate trends. The MSSA procedure initially calculates covariance after channel reduction with Principal Component Analysis (PCA), then using moving windows of 2-12 months, long enough to capture annual cycles, we recovered 80% of the signal variance in the first 20 Empirical Orthogonal Functions (EOFs), which included the seasonal cycles in the time series. In the first instance, surface motion time series were reconstructed using EOFs 1 - 6. This reconstruction captured the seasonal cycles but also included

longer-term climate trends, notably three wetter years leading to the 2018 European wide drought (Buras et al., 2020). This climate trend causes merging and shouldering of peaks that compromised the detection of the seasonal cycles, particularly in the west of the study area, where it is wetter. To overcome this difficulty, we used a surface motion time series reconstruction using EOFs 5 and 6 (Fig. 2; Supplement 1.1 Fig. S1) which extracted only the seasonal cycles. The final MSSA reconstruction provides a signal of relative movement, not absolute surface height (Fig. 2).
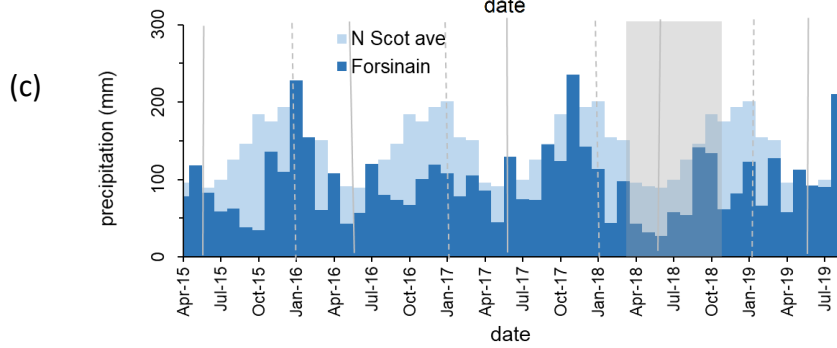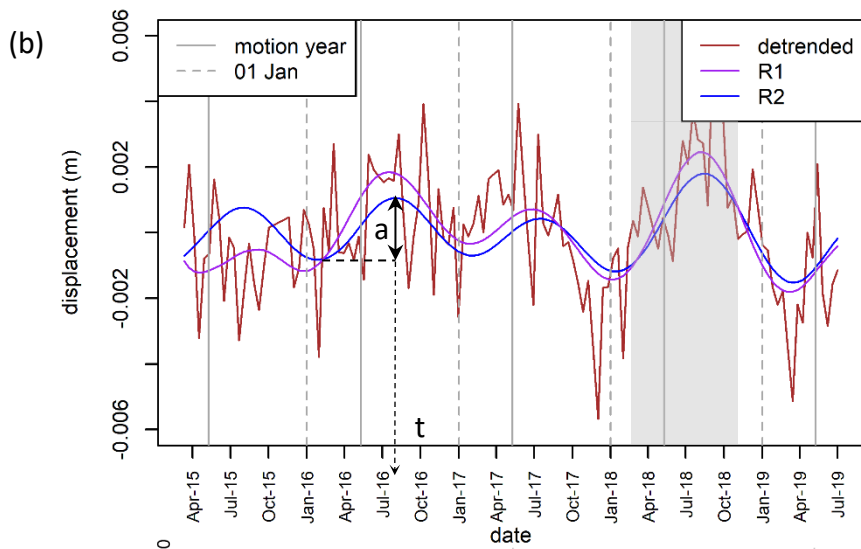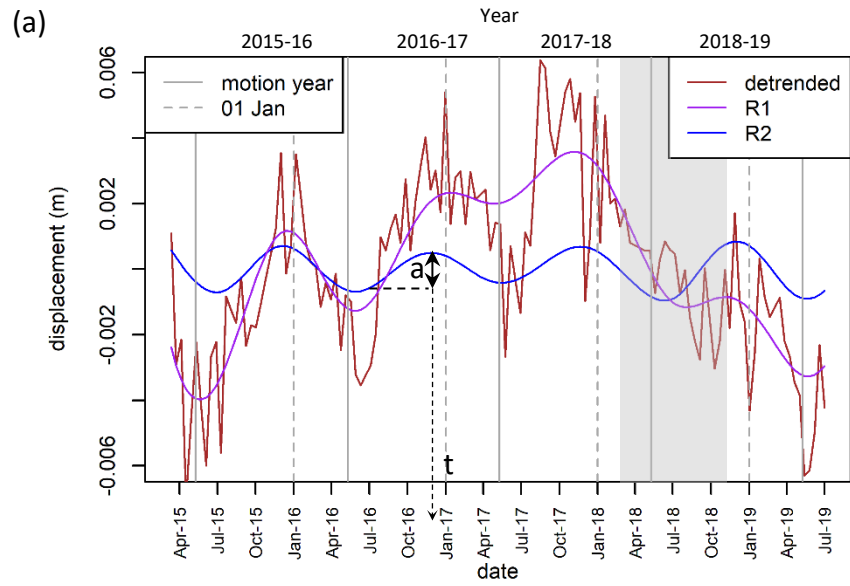
Figure 2: Examples of surface motion time series, and the metric definitions for (a) 'soft' wet bog and (b) a 'stiff' drier bog, calculated from Sentinel-1 APSIS InSAR time series data between March 12th 2015 and 01 July 1st 2019 against (c) monthly precipitation for northern Scotland (UK Met Office 20 year average, light blue) and Forsinain in the Flow Country (Scottish Environment Protection Agency, Dark blue). The initial mean detrended time series (brown), and Multichannel Singular Spectrum Analysis (MSSA) reconstructions, (R1) retaining the local climate trend (purple, a combination of empirical orthogonal functions 1 - 6) and R2 annual seasonal cycles (blue, a combination of empirical orthogonal functions 5 and 6) are shown. The two surface motion metrics used in the analysis are, peak timing (dotted line, t), and amplitude (solid line, a) shown for the surface motion year May 10th 2016 to May 9th 2017. A third surface motion metric, multi-annual average velocity is not illustrated here as it is part of the InSAR data processing (Sect. 3.1). This asynchronous timing of peaks between (a) and (b) forms a bimodal distribution in the peak amplitude timing of the peatland landscape. The drought event of 2018 (Buras et al., 2020) is shaded and can be seen to influence relative surface motion with a local climate trend in the 'soft' wet bog (a).

Third, the MSSA reconstructions were then analysed for two of three surface motion metrics used to represent the condition of the peatland within each pixel for each motion year using the R 'pracma' peak-find function (R Core Team, 2013). Metric one, the date of the annual peak 'swelling' in the seasonal cycle (peak timing) of the MSSA reconstruction within 12 months from mid-May (Fig. 2). This has been shown to relate to peatland ecohydrology (Alshammari, et al., 2020; Tampuu et al., 2020). Metric two, the annual maximum amplitude (m) in the surface motion signal (amplitude) measured from the previous seasonal minimum of the MSSA reconstruction (Fig. 2). This is an indicator of the elastic response of the peat to changes in water storage (Roulet, 1991; Waddington et al., 2010). Metric three, is the multi-annual average velocity (m yr^{-1}) of the peatland surface calculated directly and previously described from the APSIS processing. This is a measure of vertical peatland growth (greater positive value) or subsidence (greater negative value) calculated over a fixed section of the time series (Sowter et al., 2013).

As the 2018 drought caused severe and widespread subsidence, it was found to have subdued the multi-annual average velocity and for this reason, we concentrated our analysis between May 10th 2015 and May 9th 2018, discarding the drought period. Multi-annual average velocity was recalculated accordingly. While the impacts of climate anomalies on the time series were noticeable and interesting, the first step is to gain an understanding of how InSAR data can be used to characterise peatland condition, and we focus on this aspect. We also screened time series with multiple peaks per annum or years where peaks were not discernible, and these pixels were classed as having irregular cycles. Irregular time series made up 8.4% of the data set and are commonly associated with water courses and damaged bog (including agriculture and some forested pixels). Exclusion of these irregular time series does not affect our conclusions. Additionally, for the first and last years in the time series (2014 to 2015 and 2018 to 2019) as many surface motion time series are truncated preventing the accurate calculation of amplitude or peak timing in those years the mapping can be incomplete, so for clarity we show most results for 2016 to 2017. To understand the relationships between the three metrics with respect to peatland condition we visualised the metrics in a 3-axis plot.

3.2 Ecohydrological classification of the sub-sites

The training bed of the sub-sites SS1 to SS5 were divided manually into 130 smaller polygons (hereafter, sub-site polygons). Polygons ranged from (0.3 to 0.6 km^2), a practical size (a) for reliable field and map-based validation and (b) to be appropriate

for capturing key features of the landscape (e.g., pool systems, forestry or restoration blocks, streams and banks). To find

170   boundaries between the polygons, one of the authors without specialist peatland knowledge searched for distinct contrasts in the landscape structure (e.g., topographic setting, natural drainage, evidence of drainage ditches and where these features would influence hydrology, forestry plantation, restoration, land management and the likely range, consistency or inconsistency in peak timing). This was possible using Google Earth, maps and the InSAR data (Supplement 1.2, Fig. S2). An additional set of 125 polygons were randomly selected across the whole study area using the ESRI ArcMap 'random point' tool (hereafter,

175   random polygons). The immediate area close to the point were similarly assessed for features in the landscape, to define the polygon boundaries (most between $0.2 – 0.5$ km^2). While the sub-sites included the continuum of conditions and features adjacent to each other, the random polygons ensured that there was an improved capture of the ecohydrological states across the whole study area, reducing the likelihood that the sub-sites may have excluded a particular ecohydrological state. Summary statistics, of the three surface motion metrics were calculated for each polygon. Average altitude, slope and aspect for all

180   InSAR points in each polygon were also calculated from the Shuttle Radar Topography Mission Digital Elevation Model (Jarvis et al., 2008) to provide measures of topography (Supplement 1.3).

The full set of polygons (sub-sites and random polygons) was then passed to one of the authors with specialist peatland knowledge and based locally for a 'blind' (i.e., without prior knowledge of, or information about InSAR metrics within the

185   polygons) ground based eco-hydrological classification. For each polygon, the cover of plant functional types (PFTs; *Sphagnum*, other mosses, shrub, sedges, grasses, rushes, and conifer trees) and the presence of hydrological features (pools, streams, drains, erosion gullies, slope), were recorded using a semi-quantitative scale, (0 = not present or scarce, 1 = present, 2 = co-dominant, 3 = dominant). Current management (conservation, drainage for agriculture and peat cutting, forestry, restoration by forest-to-bog, restoration by drain blocking, and wind-farm construction) and historical management (e.g.,

190   burning, land-use conversion including wind-farm development, and restoration), was also documented for each polygon. The author responsible for classification visited and surveyed all the sub-site polygons and 86 of the random polygons (i.e., 85% of all polygons) by walking across the polygon. For the random polygons where access was not permitted, shared local knowledge from stakeholders (land managers, project officers on the ground, wardens, and gamekeepers) was used instead of a field visit. In all cases, this was complemented with a combination of existing data, 1:50 000 UK Ordnance Survey maps,

195   NatureScot National Vegetation Classification maps (SNH, 2019), and Google Earth imagery.
Using the semi quantitative scores, the PFT and hydrology polygon attributes were clustered by similarity using a Hierarchical Cluster Analysis (HCA; Supplement 1.4, Fig. S3). To avoid an overly split hierarchical tree with only one or two members per cluster requiring complex explanation, it was deemed more informative to analyse the PFTs, hydrology and the topography categories separate from each other. For the PFTs, once the clustering was complete, the average score of the semi-quantitative

200   scale of each PTF in the cluster was ranked. The top three PFTs were used to characterize and name the plant functional group composition. Absence of a PFT was also noted to assist interpretation (Tables S1-S4). For data visualization of the results,

clusters were further grouped based on the dominant PFT, resulting in five plant functional groups: *Sphagnum*, Shrub, Grass, Bare peat (where Low or Absent vegetation was dominant) and Forestry (Table 2). The four polygons that were dominated by rushes (R) had shrub as a co-dominant vegetation, so they were incorporated into the Shrub group. While Sedges (Sg) were co-dominant in many *Sphagnum* and shrub polygons, they were not the dominant PFT in any clusters and therefore did not form a separate group.

Table 2: Percentage proportion of clusters derived from Hierarchical Cluster Analysis based on plant functional types (PFTs) represented in the polygons of the five sub-sites and the random polygons. Clusters are defined by the dominant (first) and co-dominant (subsequent) PFTs. PFT notations: Sp = *Sphagnum*, S = Shrub, Sg = Sedges, M = Moss, G = Grasses, R= Rushes, F= Forest, LoA = Low or absent vegetation (brash, bare peat following tree felling or restoration activities etc.). PFT in brackets denotes a notable presence. n=number of polygons. For data visualization, clusters were grouped based on the dominant PFTs in five plant functional groups: Sphagnum, Shrub, Grass, Bare peat and Forestry. Clusters dominated by Rushes (R) were incorporated in the shrub group for data visualization given their low number and shrub co-dominance. Bare peat and Forestry were retained despite low numbers, as their vegetation is associated to specific management intervention.

Group Name	Sub-site Clusters	SS1	SS2	SS3 %	SS4	SS5	Random Clusters	All %
Sphagnum	**Sp,S,Sg**	37.9	29.6	0	45.5	19.2	**Sp,Sg,S**	28
Shrub	**S,Sg,Sp(G)**	17.2	14.8	0	13.6	0	**S,Sg,M/ Sp**	28
	S,Sg,R	10.3	48.1	3.8	4.5	34.6	**S,Sg,G,M**	8
	S,Sg,M	20.7	0	69.2	9.1	0	**S,G,R**	8
	S,Sg,M(G)	3.4	0	23.1	18.2	0		
	R,S	0	0	0	0	3.8	**R,Sg,S**	4
Grass/ rushes	**G,S,R**	10.3	3.7	0	4.5	11.5	**G,R,S, nSp,nM**	8
	G,R	0	0	0	4.5	11.5	**G,S,R**	1.6
Bare	**LoA**	0	0	0	0	7.7	**LoA**	4
Forest	**F**	0	3.7	3.8	0	3.8	**F**	9.6
	n=	*26*	*27*	*26*	*22*	*29*	***n=***	*125*

We also categorized topography into equal altitude belts, 0-150 m, 151-300 m and 301-450 m, and split slope face direction into four quadrants (north, east, south and west facing) and ran the HCA. Except for the highest most eroded SS3 site, altitude

220 and aspect did not show any meaningful cluster groups and played no further part in the analysis. The lack of topographic relationships are largely due to the gentle relief of the Flow Country that has few sheltered slopes and deep valleys. Instead, we used average gradient (degrees) in the polygon and found a natural breakpoint at 1.5 degrees that split the dataset equally between Flat (< 1.5 degrees) and Slope (>1.5 degrees).

3.3 Mapping the state of the peatland system

Within the 3-axis plot, we then chose a point with a winter peak timing, a high amplitude and extreme positive velocity, normally associated with 'soft' wet, *Sphagnum* peat and mapped the whole study area relative to that point. The actual reference point was selected by isolating the points that peaked in the winter, then stepping down through the percentiles of the metrics distributions until the case with the most frequent timing (e.g., February), highest positive velocity (e.g., 0.006 m yr-1) and

230 highest amplitude (e.g., 0.008 m) was identified. For the condition mapping, data for all other points in the 3-axis plot were then paired with this reference point and the Euclidian distance between them in 3-dimensional (Cartesian) space was calculated. Based on the subsequently observed bimodal distributions (Sect. 4; Fig. 3), if the paired point was in the opposite side of the bimodal distribution to the reference point, the Euclidian distance was mapped as a 'V' shaped path via zero velocity and zero amplitude at the mid date, 10th November, between the earlier and later timed clusters in the distribution. Prior to

235 calculation, the positions of the outer portions of the 3-axis plot were adjusted. This is because if the paired point is before (left of) the earlier peak and after (right of) the later peak the difference between the peak timing and the origin would be overestimated. To mitigate this, these cases were folded inwards along the axis of the peak of their distributions (effectively turning the upturned 'W' shape of the bimodal distribution into an 'M' shape). Using the natural breaks (Jenks) classification in ESRI ArcGIS as a guide, thresholds were used to classify distance from the 'soft' wet Sphagnum point. These values were

240 then mapped to produce an ecohydrological classification across the whole study site.

To further validate our ecohydrological classification map, we remotely identified and marked the central locations of all the pool systems within the study area (328 in total) using Google Earth images and determined if these markers corresponded to the 'soft' wet Sphagnum state. Although 'soft' wet areas in which *Sphagnum* is dominant do not necessarily contain pool systems, pool systems in this area almost always contain 'soft' wet peat. Furthermore, in the study area, pool systems provide

245 a spatially distributed, abundant and easily identifiable sample of this part of the peatland system. They also correspond to the part of peatland systems most unequivocally associated with 'near-natural' ecohydrological condition in this type of upland blanket bog. As the position of each pool marker did not take into account that pool systems often display complex morphology, varying geometries (and sometimes variable condition) related to local hydrological conditions (Goode, 1973; Lindsay, 2016) there was a need to tolerate a level of spatial uncertainty. To capture this, a wider area of 150m (using the buffer function in

250 ESRI ArcMap) was calculated around the marker. This buffer area contained at least 3 by 3 pixels of the ecohydrological map.

We then calculated the percentage of pixels identified in the ecohydrological classification as 'soft' in the buffer. Pixels classed as irregular were not included in the count (Table S5). We acknowledge that we focus on one particular state of peat, which does not account for the presence of drier, thin or damaged peat conditions. Indeed, stiffer, thin and damaged peat cannot readily be associated with a single, well-defined and remotely identifiable feature distributed across the whole study area in the same way. For instance, whilst drains can be observed from Google Earth, their age, maintenance and the extent of their impact on the peat would require further evidence beyond the scope of this study.

4 Results

From the frequency histograms of maximum peak timing, we discovered a bimodal distribution, showing an early and late peak (Fig. 3a), and defined the motion year to begin at the least active swelling period on May 10th to avoid dividing periods of maximum swelling into consecutive calendar years. The bimodal distribution peaks fall between August to October and December to February, similarly illustrated in the 3-axis plots (Fig. 3b-f). For each of the sub-sites, the plots of the three motion metrics show small variations on the shape and position of the data cluster reflecting the diversity of peatland conditions sampled across the landscape.

265
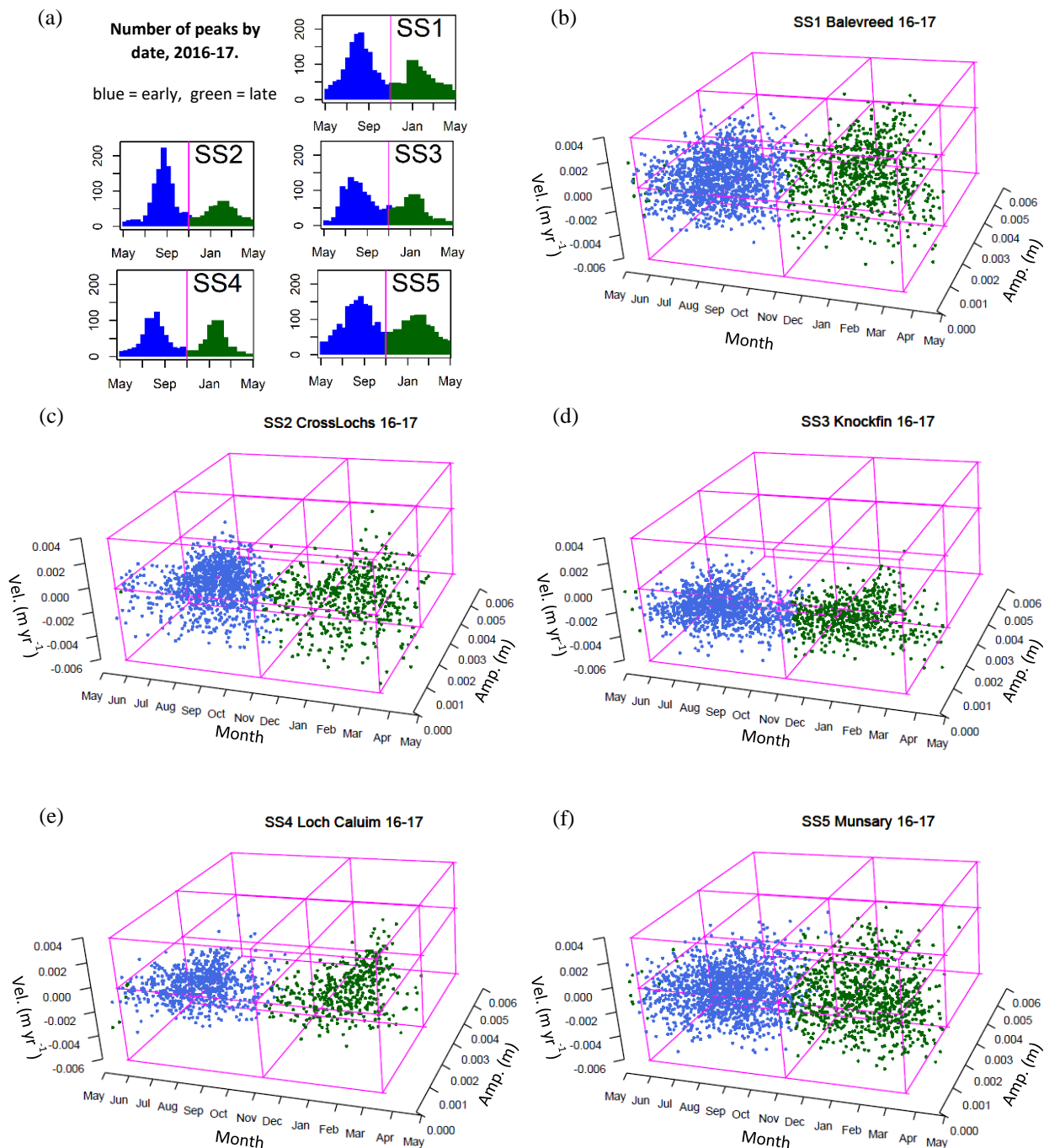
Figure 3: Characteristics of the motion metrics by Sub-Site (SS) calculated from MSSA reconstructions of the InSAR detected annual motion between May 10th 2016 to May 9th 2017. (a) Frequency of peak timing throughout the motion year where May is the

period of least surface motion activity, with a binomial distribution split at 10th November into an early (blue) and late (green) cluster. (b to f) 3-axis plots of the surface motion metrics, (b) SS1 Balavreed, (c) SS2 Cross Lochs, (d) SS3 Knockfin Heights, (e) SS4 Loch Caluim, (f) SS5 Munsary. Axis: x, peak time (Month); y, amplitude (Amp.: m), z, multi-annual average velocity (Vel.: m yr^{-1}). For multi-annual average velocity, greater +ve is peatland growth and greater –ve is peatland subsidence. Magenta box is for visual reference. Each sub-site demonstrates a specific range in peatland condition according to the plot space they occupy.

4.2 Relationship between surface motion and eco-hydrology

The HCA revealed ecological groups relating to dominant plant functional types that were comparable between the sub-site and random polygons (Table 2) as well as hydrological groups separating polygons with pool systems and polygons with streams from all other polygons (Fig. S3). When the HCA classifications and topographic information (slope) were compared to the surface motion metrics, we determined the following consistent relationships for the sub-site and random site polygons:

4.2.1 Timing, hydrology and topography

Shifts in the peak timing distributions relate to a combination of topography, hydrology, and plant functional group (Fig. 4), and peak timings themselves were consistent within groups between the three motion years. *Sphagnum*-dominated polygons are almost exclusively associated with Pools and more so on Flat ground with a tendency to have a peak later in the year than the most other hydrological and topographical combinations of vegetation or hydrological features. Within the hydrological class Pool, polygons with topographic gradients greater than 1.5° (Slope) for both random and subsite polygons, have their highest peak timing frequencies earlier in September and October than polygons with topographic gradients less than 1.5° (Flat), which tend to peak in November, January and February. The steeper gradients, in both random and sub-sites, tend to be associated with shrubs and grass-dominated vegetation communities with low frequencies of *Sphagnum* dominated polygons. Polygons with pools as the dominant hydrological feature tend to have their highest frequencies from October onwards, later than polygons classed as stream or polygons with other features (drainage ditches, peat cutting or erosion gullies).
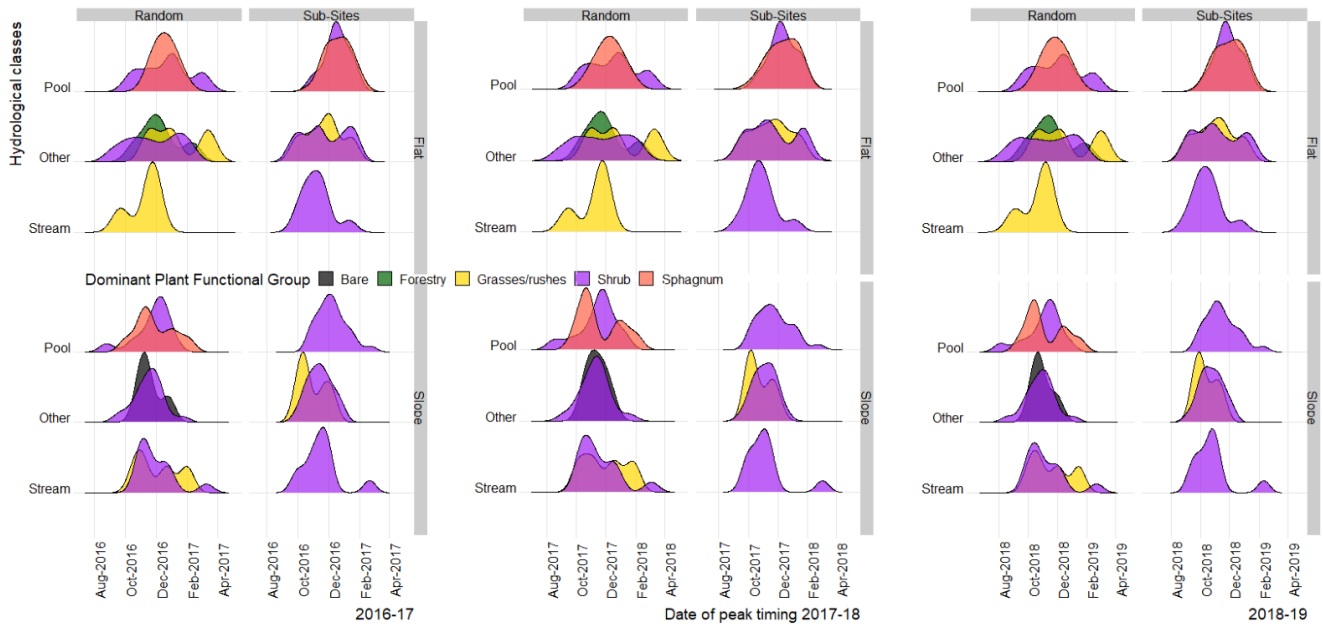
290

Figure 4: Distribution of mean peak timing date by dominant plant functional clusters for polygons with Pools, Streams or Other hydrological features (e.g., drains, erosion gullies, peat cutting, or no apparent features) in either a Flat (gradient < 1.5°) or Slope (gradient > 1.5°) topographic setting for the Random and Sub-site polygons. Plant functional group polygons (*n* random/subsite):

295 **Bare = bare peat (6/2), Forestry = conifer plantation (12/3), Grasses/rushes = grass-dominated communities (13/14), typically *Molinia caerulae*, Shrub = shrub dominated communities (59/77), typically *Calluna vulgaris* and/or *Erica tetralix*, Sphagnum = *Sphagnum* dominated communities 35/34. Sedges, rushes and other mosses are also present, often as co-dominant species in both *Sphagnum* and Shrub communities (see Table 2).**

4.2.2 Multi-annual average velocity and dominant plant functional group

Multi-annual average velocities that were most positive (gain of mass over time) were almost entirely dominated by *Sphagnum*

300 (Fig. 5). Polygons with plant functional groups typically associated with natural or man-made drainage (Shrub), disturbance (forestry and bare peat) or thin, degraded peat (Grasses) consistently displayed negative long-term multi-annual average velocities (loss of mass over time) regardless of topographical setting. Sites in which grasses or forest dominate tend to have a more intermediate multi-annual average velocity than either Shrub or *Sphagnum* dominant polygons. Where bare peat is dominant, multi-annual average velocities are lowest (most negative).

305
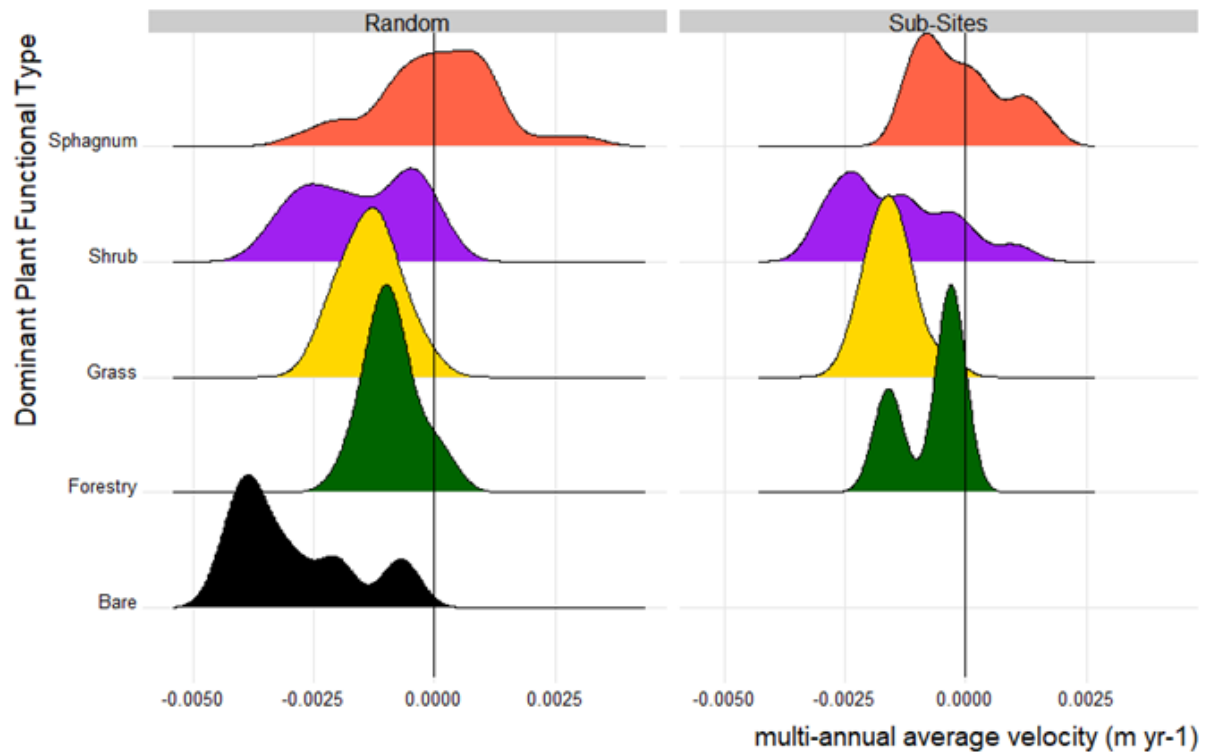
Figure 5: Distribution density of multi-annual velocity for each plant functional group and polygon type Plant functional polygons *n* (random/subsite): Bare = bare peat (6/2), Forestry = conifer plantation (12/3), Grasses/rushes = grass-dominated communities (13/14), typically *Molinia caerulae*, Shrub = shrub dominated communities (59/77), typically *Calluna vulgaris* and/or *Erica tetralix*, Sphagnum = Sphagnum dominated communities 35/34. Sedges, rushes and other mosses are also present, often as co-dominant species in both Sphagnum and Shrub communities (see Table 2).

4.2.3 Multi-annual average velocity and management

When multi-annual average velocities are compared across different management classes (Fig. 6), the least negative values are observed under conservation management and most negative values are associated with forest-to-bog management, a restoration approach that typically involves compaction from heavy machinery during the removal of conifer stands, followed by drain blocking and surface re-profiling. This restoration class shows a broader distribution in long term multi-annual average velocity than other management classes, reflecting variable degree of recovery associated with differing starting condition, time since initiation (ranging from 0 to >15 years) and techniques used in the intervention.
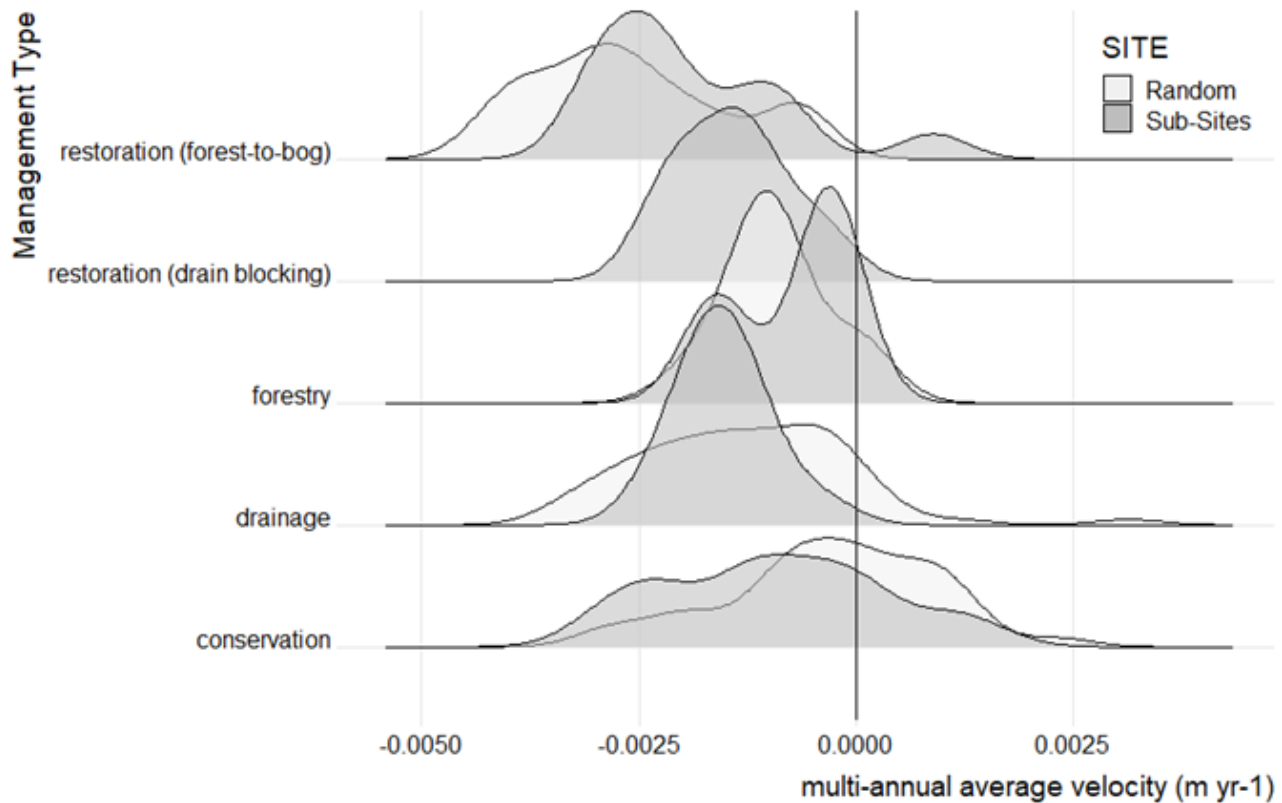
Figure 6: Distribution density of multi-annual average velocity for different management groups and by polygon type (Sub-site and random). Management polygons _n_ (Random/Sub-Site): restoration (forest-to-bog) 12/13, restoration (drain blocking) 0/6, forestry 10/3, drainage 62/13, conservation 37/95.

4.2.4 Time and magnitude of peatland swelling

The factors that influence amplitude can be deduced from relative annual amplitude change and peak timing plots for the three most dominant PFT clusters (Sphagnum, Shrub and Grass) across three surface motion years (Fig. 7). These graphs all show a positive trend between timing (day of year) and amplitude with a tendency for higher amplitudes usually occurring later in each surface motion year. Steeper slopes tend to have the lower amplitudes that peak earlier in the surface motion year. Shallow to flat slopes tend to have higher amplitudes and peak later in the surface motion year. Year-on-year variation in range of observed amplitudes is apparent, with a large range in 2015-2016 and smaller ranges in the two subsequent years. We attribute this to inter-annual variation and antecedent conditions in rainfall (e.g., Fig. 2c). A relatively dry 2014-2015 resulted in a strong amplitude response in 2015-2016 with lesser responses in the two subsequent wetter years. These differences can be related to the amount of unfilled pore space in the uppermost layer of the peat. In essence, as the peat gets wetter and the pore space fills,

335   there is less capacity in the peat to add more water and the amplitude response diminishes. A more saturated state of the peatland in 2016-2017 and 2017-2018 was also noted in field observations.
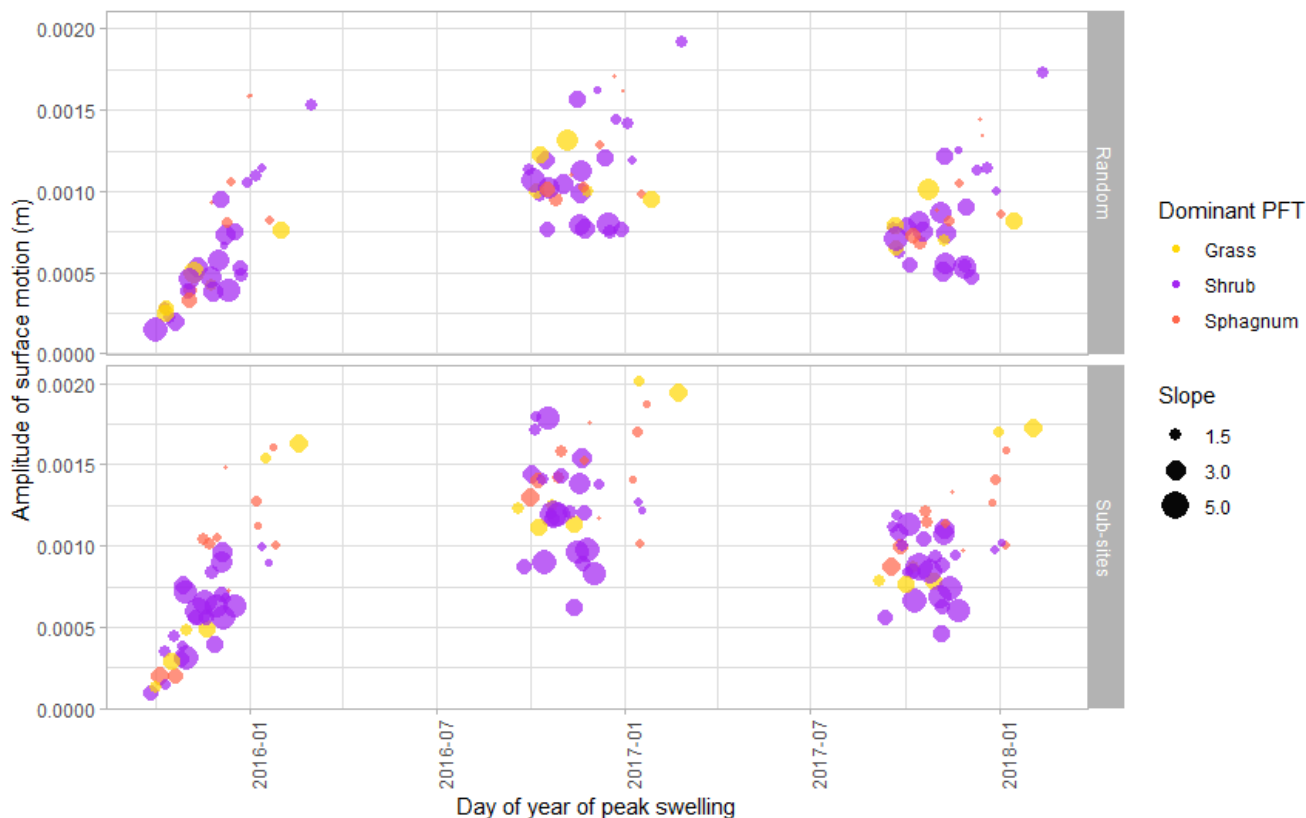
340

Figure 7: Timing of and relative amplitude for three consecutive years (2015-2018) with respect to slope gradient (degrees), dominant plant functional type (PFT; Grass, Shrub and *Sphagnum*), and by polygon type (Sub-site and random).

4.3 Application to large area condition mapping

The observed relationship between surface motion metrics and ecohydrology is readily interpreted in the context of reported

345   field measurements of peat surface motion (Howie and Hebda, 2018; Morton and Heinemeyer, 2019). Flatter sites under near natural conditions are poorly drained, wetter and dominated by *Sphagnum* spp. In turn, *Sphagnum* spp. have a considerable capacity for water storage as a direct result of their physiology (Kellner and Halldin, 2002), resulting in peak water storage and seasonal swelling of the surface later in the year. Drier sites with compacted peat have less capacity to store water and reach water holding capacity earlier in the autumn (Price, 2003). Furthermore, the more degraded peat in these sites is less

350 elastic and therefore exhibits a lower amplitude response to changes in water storage (Holden et al., 2004; Lui and Lennartz, 2019). As the seasonal water balance shifts, drier, better drained sites lose water first followed by the *Sphagnum* sites which may continue to swell on account of a hysteresis during the first stages of water loss (Howie and Hebda, 2018). Synthesizing Sect 4.2 (Fig. 4-7) the bimodal distribution of peatland surface motion timing within our landscape may be interpreted as reflecting two dominant components of the landscape. Wetter, flatter sites, typically dominated by *Sphagnum* and sedges are

355 'soft' peats, they tend to reach peak surface heights later in the year (December to February window), have higher amplitudes and more positive velocities. Drier shrub and grass dominated sites are 'stiff' peats, they tend to reach peak surface heights earlier in the year (August to October window), with slightly (but not exclusively) lower amplitude oscillations and more negative velocities. Additionally, in the 3-axis plot there are points characterized by both low amplitudes, negative velocities, and peak timings that can also fall outside the window of the 'soft' and 'stiff' class. These subtle variations of the metrics

360 identified a third broad ecohydrological class which reflects thin peats, the most degraded and drained grass dominated sites or sites under restoration that are in transition to either a 'soft' or 'stiff' state.

Mapping and applying thresholds to the Euclidian distance calculations into these three broad peatland classes relative to the 'soft' peat condition generated the peatland condition map (Fig. 8a). The classification produced patchwork of conditions in the Flow Country and the map evidences the widespread occurrence of the 'stiff' peat condition associated with both naturally

365 drier areas on the slopes and wet 'soft' peat margins but also areas made drier by land use history of burning and drainage. The impact of restoration activities, following the felling of forestry on deep peat in the last 25 years can also be seen: recent forest-to-bog clearance is displayed as 'thin/modified' peat whilst areas well on their way to recovery are showing as either the 'soft' or 'stiff' condition (Fig. 8b-c). In polygons where forest is planted on peat, the signal is much more mixed with a greater proportion of the irregular class. This mixture is a result of the poorer SAR response over trees and the variable

370 conditions encountered within forest stands. For example, in these forestry plantations, fire breaks, gaps between blocks (termed 'rides') and riparian areas that were never planted can still be wet, 'soft' and *Sphagnum* rich in contrast with the planted blocks themselves. Furthermore, plantations may enclose areas of deep peat with pools, and may display variable wetness and dryness depending on site and topography.

(a)

(b)

(c)

(d)
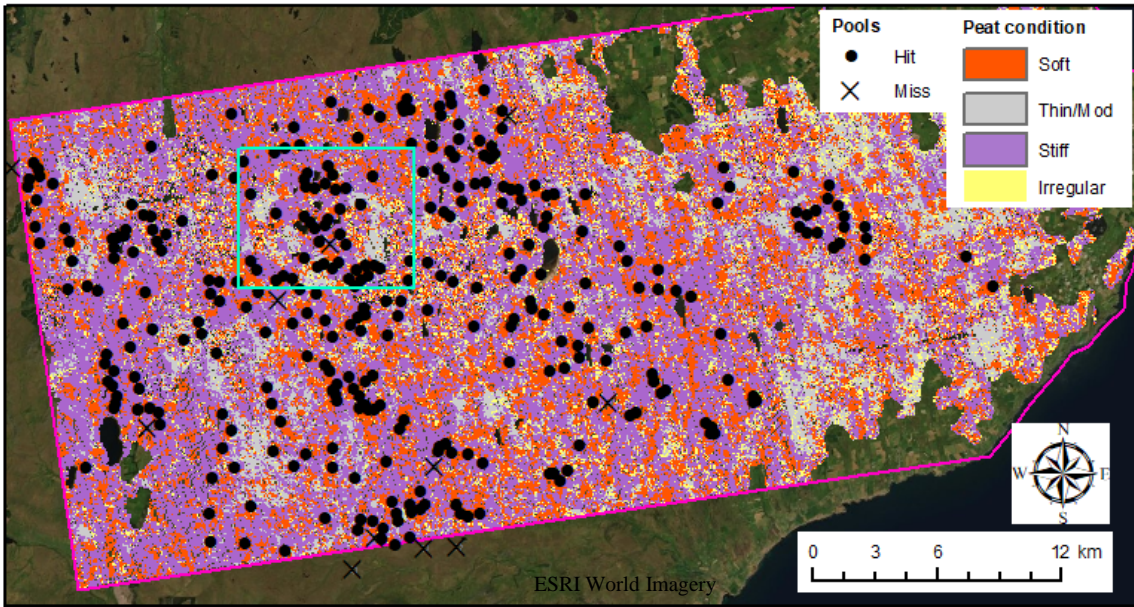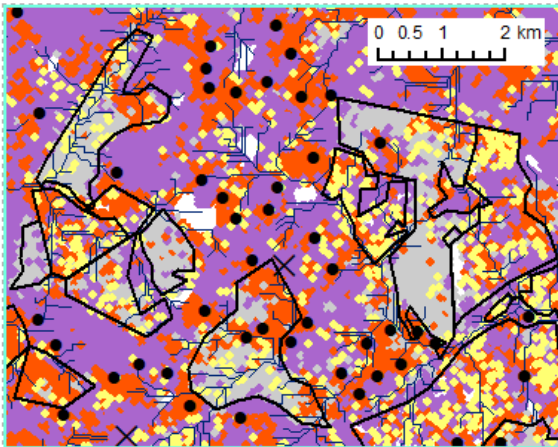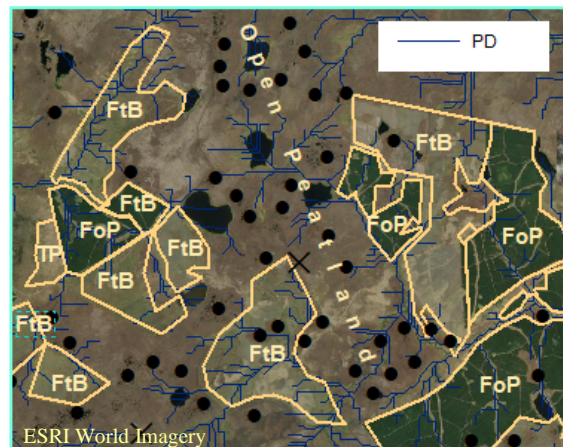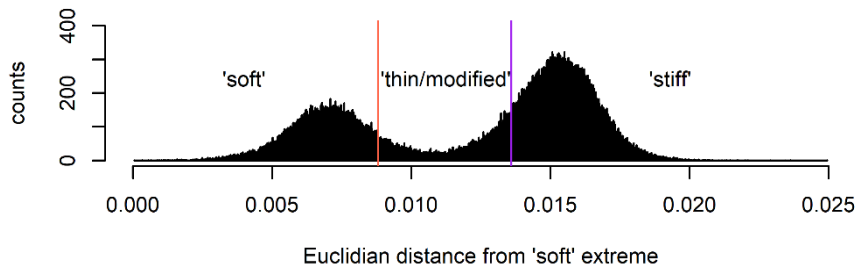
Figure 8: The ecohydrological classification of 'soft', 'thin/modified', and 'stiff' peatland condition, with respect to the location of pool systems, and areas of forest-to-bog restoration in the study area. (a) Classified map based on the Euclidian distance (in 3-dimensional Cartesian space) from the position of the 'soft' reference to all other points in the 3-axis plot of peak timing, amplitude and multi-annual average velocity, including the screened irregular time series for the period June 2016 to May 2017. Pool systems that have been correctly classified are shown as a 'hit' otherwise as a 'miss'. (b) A detailed view of the classified area highlighted within (a) illustrating the relationship with hydrology, determined from a DEM (potential drainage, PD) and polygons delineating areas for restoration. (c) A true colour satellite image of area showing the restoration status of the polygons, un-felled forest on peat (FoP), peat areas at various stages or different years of forest to bog (FtB) restoration and an area of thin peat (TP) (d) Frequency distribution of Euclidian distance, and the thresholds used to differentiate the three peat conditions. Credits: The classified area (approx. 930 km^2) was delineated using peat soils from the National Soil Map of Scotland (JHI, 2021). Images sourced via ESRI ArcMap in 2021. Image source for (a) and (c) ESRI World Imagery: Esri, DigitalGlobe, GeoEye, i-cubed, USDA FSA, USGS, AEX, Getmapping, Aerogrid, IGN, IGP, swisstopo, and the GIS User Community.

Using the criteria for the remote validation that pool systems should always fall in the 'soft' peat category, 97.9 % of the pool system markers were identified to have occurred within 150 m of that class. Detailed inspection of the remaining 2.1% (7/328) of pool system markers that did not fall within our threshold reveals that these pool systems all showed evidence of localized erosion or drainage causing degradation of their natural hydrology. While not validated in the same way, further inspection of our classification combined with specialist knowledge of the area indicates that the thin/modified class corresponds to areas under restoration, notably areas recently felled for forest-to-bog restoration, areas subject to intensive grazing, thin peat soils on steeper higher ground and in valley bottoms (e.g., Fig. 8b-c). The abundance of the 'thin/ modified' class is striking in the east of the study area and we note that this corresponds to long-term historical usage of the land for agriculture and associated cutting of peat for fuel (Andersen et al., 2018; Minasny et al., 2019).

Within the area, our method identifies approximately 254 km^2 (27.3 % of the area) as 'soft' wet *Sphagnum* dominated peat, 481 km^2 (51.7 %) as 'stiff' shrub dominated peat, 117 km^2 (12.8 %) as the 'thin/modified' peat class with 78 km^2 (8.4 %) as irregular time series. This classification therefore provides an overall measure of the current state of this blanket bog landscape, to which future regional change, on account of climate change or restoration, may be compared.

5 Discussion

Our most important finding is that surface motion metrics derived from APSIS InSAR time series enable almost continuous spatial and temporal characterization of peatland condition at large scales. That the SAR data can penetrate cloud cover, measures regular physical displacement of the surface, and captures a known dynamic behaviour associated with peat resilience gives this approach a significant lead over the far more challenging effort to measure peatland condition from optical reflectance data (e.g. Artz et al., 2019). This is compounded by the fact that peatland areas are often obscured by cloud

(Minasny et al., 2019). A valuable exercise would be to quantify the similarities and contrasts of motion mapped peatland condition to optical products and we anticipate that motion data will bring different and complementary information. This may be advantageous for restoration monitoring and information on peatland mechanical condition from surface motion may be key to resolving weaknesses in optical studies, for example in carbon accounting (Couwenberg et al., 2011).

415 The sensitivity and dynamic response of surface motion metrics to changes in the state of the peatland system should make the method ideally suited to monitoring and informing peatland management and restoration. Globally, large areas of northern peatlands degraded by historic drainage, grazing and forestry are now under or targeted for restoration (Rochefort et al., 2017). Consequently, peatland conservation and restoration are increasingly perceived as critical tools in the fight against global climate change (Leifeld and Menichetti, 2018; Amelung et al., 2020; Günther et al., 2020). Restoration strategies typically

420 involve raising water levels to re-establish wet conditions. The expectation is that this will promote *Sphagnum* establishment, often a key measure of the success of an intervention (Rochefort et al., 2017; Bellamy et al., 2012; Caporn et al., 2018; González and Rochefort, 2019).

In the case of blanket bog landscapes, our finding of naturally 'stiff' drier shrub and 'soft' wetter *Sphagnum* states raises the question as to whether a strategy of increasing *Sphagnum* cover is always an appropriate restoration target, or indeed if it is

425 the only desirable outcome for blanket bogs. In this context, an APSIS InSAR-based assessment of the condition of a whole blanket bog landscape can help guide restoration strategies by first identifying the typical natural states and hydrological structure of that landscape. Second, following intervention, this approach could enable a robust monitoring of restoration trajectories and outcomes (Marshall et al., 2020). Our study also suggests that when monitoring restoration trajectories over time, the impacts of interannual variabilities such as precipitation on the metrics would likely need to be accounted for.

430 In natural landscapes, these peatland states are a consequence of landscape evolution in which the vertical accumulation of peat must be counterbalanced on an appropriate spatial and temporal scale by erosion (Large et al., 2021). Drier states correspond to areas of net carbon loss due to natural drainage, incision and erosion along peatland margins, and wetter states correspond to peatland interiors, areas with low gradient, that tend towards carbon accumulation. In this context, to restore a site that is naturally 'stiff' and dry to the 'soft' wet state would risk instability, while the opposite would fail to optimize carbon

435 storage. A more suitable and sustainable ambition is to accept that restored blanket bog sites may follow different trajectories towards naturally *Sphagnum* or shrub states (or 'soft' and 'stiff'), and that these target end states will be constrained by the hydrological landscape setting, as conceptualized by Winter (Winter, 1988). Our approach provides evidence for these natural states co-existing within the study areas, and evidence to guide and monitor appropriate restoration trajectories within this system. Recognizing and preserving this mosaic is critical in maintaining large- and small-scale peatland landscape stability

440 and carbon balances, particularly as long-term models suggest that the natural drying out of peatland is accelerating due to drainage (Harris et al., 2020; Leifeld et al., 2019) and climate change (Gallego-Sala and Prentice, 2013).

The approach outlined here should be readily transferable to alternative peatland settings within different parts of the global peatland climate space. Using surface motion metrics identified from the InSAR time series of peatland motion, a surface

deformation space for a given peatland system can be defined. The position of ecohydrological characteristics within this space can then be deployed to quantify the state of the peatland system and map changes with respect to climate change and management intervention. This capacity to customize the approach is valuable as it provides the means to measure peatland condition at a global scale. If realized, this would enhance our understanding of the large-scale functionality of peatland landscapes and provide the robust evidence base required for sustainable peatland management.

Data availability

doi: 10.17639/nott.7123

Supplement Link

Supplement supplied

Author Contribution

A.S. led the processing of the InSAR data that A.V.B. post-processed, analyzed and visualized. R.A. recorded the polygon attributes, mapped the pools, contributed to data visualization and completed the ground surveys with C.M. D.J.L developed the overall idea of applying InSAR for this purpose. All authors were responsible for critical contributions, passing the final manuscript and editing text and figures.

Competing Interests

Andrew Sowter is affiliated with Terra Motion Limited. The APSIS (Advanced Pixel System using Intermittent SBAS) method is owned by the University of Nottingham and is the subject of a UK Patent Application (No. 1709525.8) with the inventor named as Dr. Andrew Sowter; it is currently Patent Pending.

Disclaimer

We are not responsible for the consequences of any decisions or actions even if they have been influenced by the material and ideas in this manuscript.

Acknowledgments

The authors would like to thank members of the following organizations who provided access to sites for surveys or insight and local knowledge about past and present management over the study area: NatureScot Peatland ACTION, Royal Society for the Protection of Birds, Plantlife Scotland, Forestry and Land Scotland, Scottish Forestry, Welbeck Estate and Shurrery Estate. David Gee and Ahmed Athab for their assistance with the APSIS InSAR data output. "National Soil Map of Scotland" copyright and database right The James Hutton Institute v.1_4. Used with the permission of the James Hutton Institute. All rights reserved. Any public sector information contained in these data is licensed under the Open Government License v.2.0. R.A. and C.M are funded by a Leverhulme Leadership Award (1466NS) and D.J.L, R.A. and C.M. with a NERC InSAR TOPS NE/P014100/1.

References

Alshammari L., Large D.J., Boyd, D.S., Sowter S., Anderson R., Andersen R., and Marsh S.: Long-term peatland condition assessment via surface motion monitoring using the ISBAS DInSAR technique over the Flow Country, Scotland. Remote Sens., 10, 1-24, doi:10.3390/rs10071103, 2018.

Alshammari, L., Boyd, D.S., Sowter, A., Marshall, C., Andersen, R., Gilbert, P., Marsh, S., and Large, D.J.: Use of surface motion characteristics determined by InSAR to assess peatland condition, J. Geo. Res: Biogeosciences, 125, e2018JG004953, doi:10.1029/2018JG004953, 2020.

Andersen, R., Cowie, N., Payne, R.J., and Subke, J.A.: The Flow Country peatlands of Scotland. Mires and Peat, 23, 1-2, doi:10.19189/MaP.2018.OMB.381, 2018.

Almendinger, J.C., Almendinger, J.E., and Glaser, P.H.: Topographic fluctuations in across a spring fen and raised bog in the Lost River Peatland, northern Minnesota. J. Ecol., 74, 393-401, doi:10.2307/2260263, 1986.

Amelung, W., Bossio, D., de Vries, W., Kögel-Knabner, I., Lehmann, J., Amundson, R., Bol, R., Collins, C., Lal, R., Leifeld, J. and Minasny, B.: Towards a global-scale soil climate mitigation strategy, Nat. Comms., 11(1), 1-10, doi:10.1038/s41467-020-18887-7, 2020.

Artz, R.R.E.; Johnson, S.; Bruneau, P.; Britton, A.J.; Mitchell, R.J.; Ross, L.; Donaldson-Selby, G.; Donnelly, D.; Aitkenhead, M.J.; Gimona, A.; Poggio, L.: The potential for modelling peatland habitat condition in Scotland using long-term MODIS data., Sci. Tot. Env, 660, 429-442, 2019.

Baden, W., and Eggelsmann, R.: Der Wasserkreislauf eines nordwestdeutschen Hochmoores. Verleg Wasser und Boden, Hamburg, Germany, 1964.

Bateson, L., Cigna, F., Boon, D. and Sowter, A.: The application of the Intermittent SBAS (ISBAS) InSAR method to the South Wales Coalfield, UK. Int. J. App. Earth Obs. Geoinform., 34, 249–257, doi:10.1016/j.jag.2014.08.018, 2015.

Becker, R. A., Chambers, J. M., and Wilks, A. R.: The New S Language. Wadsworth & Brooks/Cole, 1988.

Bellamy, P.E., Stephen, L., Maclean, I.S., and Grant, M.C.: Response of blanket bog vegetation to drain-blocking. Appl. Veg. Sci., 15(1), pp.129-135, doi:10.1111/j.1654-109X.2011.01151.x, 2012.

Box, G.E.P. and Cox, D.R.: An Analysis of Transformations. J. R. Stat. Soc. B Methodol., 26(2) 211-252 (1964).

Buras, A., Rammig, A., and Zang, C.S.: Quantifying impacts of the 2018 drought on European ecosystems in comparison to
500   2003. Biogeosciences, 17(6), 1655-1672, doi:10.5194/bg-17-1655-2020, 2020.

Caporn, S.J.M., Rosenburgh, A.E., Keightley, A.T., Hinde, S.L., Riggs, J.L., Buckler, M. and Wright, N.A.: Sphagnum restoration on degraded blanket and raised bogs in the UK using micropropagated source material: a review of progress. Mires and Peat, 20, 1-17, doi:10.19189/MaP.2017.OMB.306, 2018.

Chen, C.W., and Zebker, H.A.: Two-dimensional phase unwrapping with use of statistical models for cost functions in
505   nonlinear optimization. J. Opt. Soc. Am. A, 18, 338–351, doi:10.1364/JOSAA.18.000338, 2001.

Cigna, F., and Sowter, A.: The relationship between intermittent coherence and precision of ISBAS InSAR ground motion velocities: ERS-1/2 case studies in the UK. Remote Sens. Environ., 202, 177–198, doi:10.1016/j.rse.2017.05.016, 2017.

Crump J. (Ed.), Smoke on water: Countering global threats from peatland loss and degradation. UNEP, GRIDA, GPI, 2017.

S.Fiaschi, E.P. Holohan, M. Sheehy, M. Floris, PS-InSAR Analysis of Sentinel-1 Data for Detecting Ground Motion in
510   Temperate Oceanic Climate Zones: A Case Study in the Republic of Ireland. Remote Sens., 11(3), doi:10.3390/rs11030348, 2019.

Couwenberg, J., Thiele, A., Tanneberger, F., Augustin, J., Bärisch, S., Dubovik, D., Liashchynskaya, N., Michaelis, D., Minke, M., Skuratovich, A., and Joosten, H.: Assessing greenhouse gas emissions from peatlands using vegetation as a proxy. Hydrobiologia volume 674, 67–89, https://doi.org/10.1007/s10750-011-0729-x, 2011.

515   Fritz, C., Campbell, D.I., and Schipper, L.A.: Oscillating peat surface levels in a restiad peatland, New Zealand – magnitude and spatiotemporal variability. Hydrol. Processes. 22, 3264-3274 doi: 10.1002/hyp.6912, 2008.

Glaser P.H., Chanton J.P., Morin P., Rosenberry D.O., Siegel D.I., Ruud O., Chasar L.I., and Reeve A.S.: Surface deformations as indicators of deep ebullition fluxes in a large northern peatland. Global Biogeochem. Cycles 18, GB1003, doi:10.1029/2002GB002069, 2004.

520   Gallego-Sala, A.V., and Prentice, I.C.: Blanket peat biome endangered by climate change. Nat. Clim. Change. 3(2), 152-155, doi:10.1038/nclimate1672, 2013.

Ghil M., Allen M. R., Dettinger M. D., Ide K., Kondrashov D., Mann M. E., Robertson A. W., Saunders A., Tian Y., Varadi F., and Yiou P.: Advanced spectral methods for climatic time series. Rev. Geophys. 40, 1-40, doi:10.1029/2000RG000092, 2002.

525   Gong, W., Thiele, A., Hinz, S., Meyer, F.J., Hooper, and A., Agram, P.S.: Comparison of small baseline interferometric SAR processors for estimating ground deformation. Remote Sens. 8, 330, doi:10.3390/rs8040330, 2016.

González, E., and Rochefort, L.: Declaring success in Sphagnum peatland restoration: Identifying outcomes from readily measurable vegetation descriptors. Mires and Peat. 24(19), 1-16, doi:10.19189/MaP.2017.OMB.305, 2019.

Goode, D.A.: The significance of physical hydrology in the morphological classification of mires. Classification of Peat and Peatlands. In Proc Int. Peat Soc. Symp., Eds. International Peat Society, Glasgow. pp10–20, 1973.

Günther, A., Barthelmes, A., Huth, V., Joosten, H., Jurasinski, G., Koebsch, F. and Couwenberg, J.: Prompt rewetting of drained peatlands reduces climate warming despite methane emissions, Nat. Comms., 11(1), 1-5, doi:10.1038/s41467-020-15499-z, 2020.

Hancock, M.H., England, B., and Cowie, N.R.: Knockfin Heights: a high-altitude Flow Country peatland showing extensive erosion of uncertain origin. Mires & Peat. 23, 1-20, doi:10.19189/MaP.2018.OMB.334, 2018.

Harris, L.I., Roulet, N.T., and Moore, T.R.: Drainage reduces the resilience of a boreal peatland. Environ. Res. Commun. 2(6), p.065001, doi:10.1088/2515-7620/ab9895, 2020.

Holden, J., Chapman, P.J., and Labadz, J.C., Artificial drainage of peatlands: hydrological and hydrochemical process and wetland restoration. Prog. Phys. Geogr. 28, 95–123, doi:10.1191/0309133304pp403ra, 2004.

Howie, S.A., and Hebda, R.J.: Bog surface oscillation (mire breathing) a useful measure in raised bog restoration. Hydrol. Process., doi: 10.1002/hyp.11622, 2018.

Hutchinson, J. N.: The record of peat wasteage in the East Anglian fenlands at Holme Post, 1848-1978 A.D. J. Ecol., 68, 229-249, 1980.

Hyndman, R., Athanasopoulos, G., Bergmeir, C., Caceres, G., Chhay, L., O'Hara-Wild, M., Petropoulos, F., Razbash, S., Wang, E. and Yasmeen, F.: Forecast: Forecasting functions for time series and linear models. R package version 8.5. URL:http://pkg.robjhyndman.com/forecast, 2019.

Jarvis, A., Reuter, H.I., Nelson, A., and Guevara, E.: Hole-filled seamless SRTM data V4, International Centre for Tropical Agriculture (CIAT), available at http://srtm.csi.cgiar.org, 2008.

JHI, The James Hutton Institute, "National Soil Map of Scotland" available at https://www.hutton.ac.uk/learning/natural-resource-datasets/soilshutton/soils-maps-scotland. Last accessed 22 Nov. 2021.

Kellner, E., and Halldin, S.: Water budget and surface-layer water storage in a Sphagnum bog in central Sweden. Hydrol. Process., 16(1), 87-103, doi:10.1002/hyp.286, 2002.

Kennedy, G.W., and Price, J.S.: A conceptual model of volume-change controls in the hydrology of cutover peats. J. Hydrol., 302, 13-25, doi:10.1016/j.hydrol.2004.06.024, 2005.

Kulczynski, S., Peat bogs of Polsie. Memoires de l'Academie Polenaise des Sciences et des Lettres. Class de Sciences Mathematiques et Naturelles. Serie B: Sciences Naturelles. 15, 1949.

Kurimo, H.: Surface fluctuation in three virgin pine mires in eastern Finland. Silva Fennica, 17, 45-64, 1983.

Large, D.J., Marshall, C., Jochmann, M., Jensen, M., Spiro, B.F. and Olaussen, S.: Time, Hydrologic Landscape, and the Long-Term Storage of Peatland Carbon in Sedimentary Basins. J. Geo. Res.: Earth. Surf., 126(3) doi:10.1002/essoar.10503762.1, 2021.

Lees, K.J., Quaife, T., Artz, R.E.E., Khomik, M., and Clark, J.M.: Potential for using remote sensing to estimate carbon fluxes across Northern peatlands: a review. Sci. Tot. Env., 615, 857874, doi:10.1016/j.scitotenv.2017.09.103, 2018.

Lees, K.J.; Artz, R.R.E.; Khomik, M.; Clark, J.; Ritson, J.; Hancock, M.; Cowei, N.; Quaife, T.:Using spectral indices to estimate water content and GPP in sphagnum moss and other peatland vegetation., IEEE Trans. Geo. and Rem. Sen., 58, 4547-4557, 2020.

Leifeld, J., and Menichetti, L.: The underappreciated potential of peatlands in global climate change mitigation strategies. Nat. Commun., 9(1), 1-7, doi:10.1038/s41467-018-03406-6, 2018.

Leifeld, J., Wüst-Galley, C., and Page, S.: Intact and managed peatland soils as a source and sink of GHGs from 1850 to 2100. Nat. Clim. Change., 9(12), 945-947, doi:10.1038/s41558-019-0615-5, 2019.

Liu, H., and Lennartz, B.: Hydraulic properties of peat soils along a bulk density gradient—A meta study. Hydrol. Process., 33(1), 101-114, doi:10.1002/hyp.13314, 2019.

Lindsay, R., Charman, D.J., Everingham, F., O'reilly, R.M., Palmer, M.A., Rowell, T.A. and Stroud, D.A.: The flow country: the peatlands of Caithness and Sutherland. D.A. Ratcliffe and P.H. Oswald Eds. (Nature Conservancy Council, Peterborough 1988), pp174. Available from Joint Nature Conservation Committee (JNCC) via http://jncc.defra.gov.uk/page-4281, 1988.

Lindsay, R.: Peatland Classification. In: Everard, M., Finlayson, C.M., Irvine, K., McInnes, R.J., Middleton, B.A., Davidson, N.C. (Eds.) The Wetland Book: I: Structure and Function, Management, and Methods. Springer Nature, Netherlands, pp.1–14., 2018.

Mahdiyasa, A.W., Large, D.J., Muljadi, B.P., Icardi, M., and Triantafyllou, S.: MPeat—A fully coupled mechanical-ecohydrological model of peatland development. Ecohydro., e2361. https://doi.org/10.1002/eco.2361 2021

Marshall, C., Bradley, A.V., Andersen, R. and Large, D.J.: Using peatland surface motion (bog breathing) to monitor Peatland Action sites. NatureScot Research Report 1269. https://www.nature.scot/doc/naturescot-research-report-1269-using-peatland-surface-motion-bog-breathing-monitor-peatland-action, 2021.

Minasny, B., Berglund, Ö., Connolly, J., Hedley, C., Vries, F. D., Gimona, A., Kempen, B., Kidd, D.,   Lilja, H., Malone, B., McBratney, A., Roudier, P., O'Rourke, S., Rudiyanto, Padarian, J., Poggio, L., Caten, A. T., Thompson, D., Tuve, C., and Widyatmanti, W.: Digital mapping of peatlands–A critical review. Earth Sci. Rev., 196, 102870, doi:10.1016/j.earscirev.2019.05.014, 2019.

Money, R.P., and Wheeler, B. D.: Some critical questions concerning the restorability of damaged raised bogs. Appl. Veg. Sci., 2(1), 107–116, doi:10.2307/1478887, 1999.

Morton, P.A., and Heinemeyer, A.: Bog breathing: the extent of peat shrinkage and expansion on blanket bogs in relation to water table, heather management and dominant vegetation and its implications for carbon stock assessments. Wetl. Ecol. and Manag., 27, 467–482 doi.org/10.1007/s11273-019-09672-5, 2019.

Mustonen, S.E., and Seuna, P.: Metsaojituksen vaikutuksesta suon hydrologiaan. Pages 1-63 in Publication 2, National Board of Waters, Finland, Water Research Institute, 1971.

Osmanoğlu, B., Sunar, F., Wdowinski, S., and Cabral-Cano, E.: Time series analysis of InSAR data: methods and trends. ISPRS J. Photogramm. Remote Sens., 115, 90–102, doi:10.1016/j.isprsjprs.2015.10.003, 2016.

Poggio, L., and Gimona, A.: National scale 3D modelling of soil organic carbon stocks with uncertainty propagation—an example from Scotland. Geoderma, 232, 284-299, doi:10.1016/j.geoderma.2014.05.004, 2014.

Price, J.S.: Role and character of seasonal peat soil deformation on the hydrology of undisturbed cutover peatlands. Water Resour. Res., 39(9) 1214, doi:10.1029/2002WR001302, 2003.

Price, J.S., and Schlotzhauer, S.M.: Importance of shrinkage and compression in determining water storage changes in peat: the case of a mined peatland. Hydrol. Process., 13 2591-2601, doi:10.1002/(SICI)1099-1085(199911)13:16<2591::AID-HYP933>3.0.CO;2-E, 1999.

R Core Team, R: A language and environment for statistical computing. R Foundation for Statistical Computing, Vienna, Austria. Available at http://www.R-project.org/, 2013.

R Core Team: 'Stats v3.6.2' R package, available at https://www.rdocumentation.org/packages/stats, 2020.

Reeve, A.S., Glaser, P.H., and Rosenberry, D.O.: Seasonal changes in peatland surface elevation recorded at GPS stations in the Red Lake Peatlands, northern Minnesota, USA. J. Geophy. Res.: Biogeosci., 118, 1616-1626, doi:10.1002/2013JG002404, 2013.

Rochefort, L., and Andersen, R.: Global Peatland Restoration after 30 years: where are we in this mossy world?. Rest Ecol., 25(2), 269-270, doi:10.1111/rec.12417, 2017.

Roulet, N.T., Surface level and water table fluctuations in a subarctic fen, Arc. Alp. Res., 23 (3), 303-310, 1991.

Sloan, T.J., Payne, R.J., Anderson, A.R., Bain, C., Chapman, S., Cowie, N., Gilbert, P., Lindsay, R., Mauquoy, D., Newton, A.J. and Andersen, R.: Peatland afforestation in the UK and consequences for carbon storage, Mires and Peat, 23, doi.org10.19189/MaP.2017.OMB.315, 2018.

SNH, available at http://gateway.snh.gov.uk/natural-spaces/index.jsp (last accessed 24/07/20), 2019.

Sowter, A., Che Amat, M., Cigna, F., Marsh, S., Athab, A., and Almshammari, L.: Mexico City land subsidence in 2014-2015 with Sentinel-1 IW TOPS: Results using the Intermittent SBAS (ISBAS) technique. Int. J. App. Earth Obs. Geo., 52, 230-242, doi:10.1016/j.jag.2016.06.015, 2016.

Sowter, A., Bateson, L., Strange, P., Ambrose, K., and Syafiudin, M.F.: DInSAR estimation of land motion using intermittent coherence with application to the South Derbyshire and Leicestershire coalfields. Rem. Sens. Lett., 4(10), 979-987, doi:10.1080/2150704X.2013.823673, 2013.

SPECTRA software: http://research.atmos.ucla.edu/tcd/ssa/guide/guide4.html, last accessed 2 May 2021

Tampuu, T., Praks, J., Uiboupin, R., and Kull, A.: Long Term Interferometric Temporal Coherence and DInSAR Phase in Northern Peatlands. Rem. Sens., 12(10), 1566, doi: 10.3390/rs12101566, 2020.

Waddington, J.M., Morris, P.J., Kettridge, N., Granath, G., Thompson, D.K. and Moore, P.A.: Hydrological feedbacks in northern peatlands. Ecohydrol., doi:10.1002/eco.14938(1), 113-127, 2015.

Waddington, J.M., Kellner, E., Strack, M., and Price, J.S.: Differential peat formation, compressibility, and water storage between peatland microforms: Implications for ecosystem function and development. Wat. Res. Res. 46, W07538, doi:10.1029/2009WR008802, 2010.

630   Winter, T.C.: A conceptual framework for assessing cumulative impacts on the hydrology of nontidal wetlands. Env. Man., 12(5), 605-620, doi:10.1007/BF01867539,1988.